WILEY

USING e-ANNOTATION TOOLS FOR ELECTRONIC PROOF CORRECTION

Required software to e-Annotate PDFs: Adobe Acrobat Professional or Adobe Reader (version 11 or above). (Note that this document uses screenshots from Adobe Reader DC.)
The latest version of Acrobat Reader can be downloaded for free at: http://get.adobe.com/reader/

Once you have Acrobat Reader open on your computer, click on the Comment tab (right-hand panel or under the Tools menu).

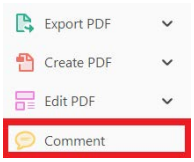

This will open up a ribbon panel at the top of the document. Using a tool will place a comment in the right-hand panel. The tools you will use for annotating your proof are shown below:

1. Replace (Ins) Tool – for replacing text.

Strikes a line through text and opens up a text box where replacement text can be entered.

How to use it:

- Highlight a word or sentence.
- Click on .
- Type the replacement text into the blue box that appears.

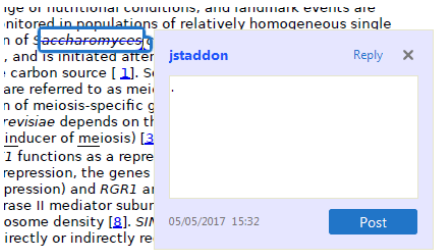

2. Strikethrough (Del) Tool – for deleting text.

Strikes a red line through text that is to be deleted.

How to use it:

- Highlight a word or sentence.
- Click on .
- The text will be struck out in red.

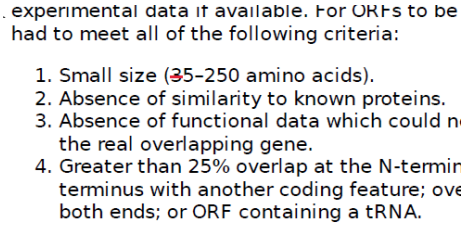

3. Commenting Tool – for highlighting a section to be changed to bold or italic or for general comments.

Use these 2 tools to highlight the text where a comment is then made.

How to use it:

- Click on .
- Click and drag over the text you need to highlight for the comment you will add.
- Click on .
- Click close to the text you just highlighted.
- Type any instructions regarding the text to be altered into the box that appears.

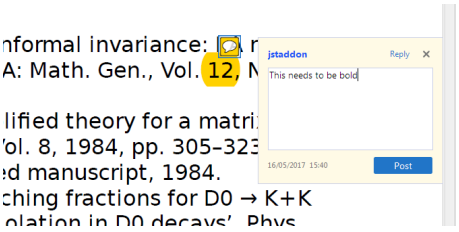

4. Insert Tool – for inserting missing text at specific points in the text.

Marks an insertion point in the text and opens up a text box where comments can be entered.

How to use it:

- Click on .
- Click at the point in the proof where the comment should be inserted.
- Type the comment into the box that appears.

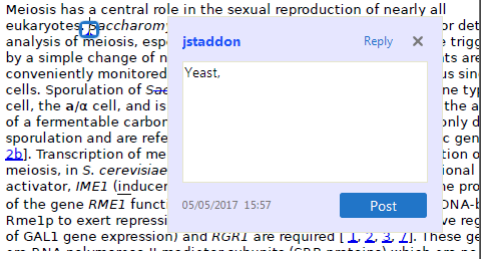

USING e-ANNOTATION TOOLS FOR ELECTRONIC PROOF CORRECTION

5. Attach File Tool – for inserting large amounts of text or replacement figures.

Inserts an icon linking to the attached file in the appropriate place in the text.

How to use it:

- Click on  .
- Click on the proof to where you'd like the attached file to be linked.
- Select the file to be attached from your computer or network.
- Select the colour and type of icon that will appear in the proof. Click OK.

The attachment appears in the right-hand panel.

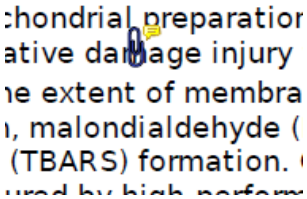

6. Add stamp Tool – for approving a proof if no corrections are required.

Inserts a selected stamp onto an appropriate place in the proof.

How to use it:

- Click on  .
- Select the stamp you want to use. (The Approved stamp is usually available directly in the menu that appears. Others are shown under *Dynamic*, *Sign Here*, *Standard Business*).
- Fill in any details and then click on the proof where you'd like the stamp to appear. (Where a proof is to be approved as it is, this would normally be on the first page).

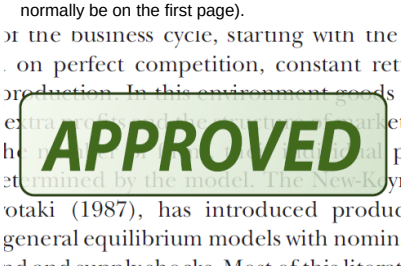

Drawing tools available on comment ribbon

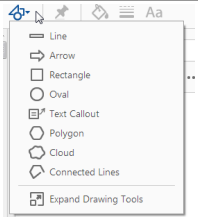

7. Drawing Markups Tools – for drawing shapes, lines, and freeform annotations on proofs and commenting on these marks.

Allows shapes, lines, and freeform annotations to be drawn on proofs and for comments to be made on these marks.

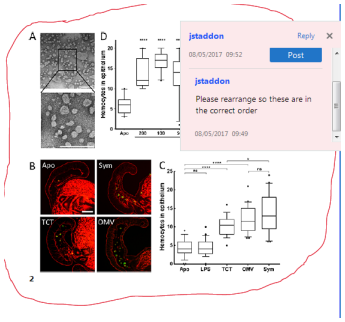

How to use it:

- Click on one of the shapes in the Drawing Markups section.
- Click on the proof at the relevant point and draw the selected shape with the cursor.
- To add a comment to the drawn shape, right-click on shape and select *Open Pop-up Note*.
- Type any text in the red box that appears.

For further information on how to annotate proofs, click on the Help menu to reveal a list of further options:

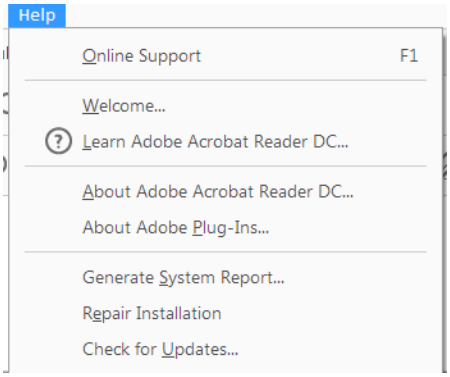

WILEY

Author Query Form

Journal: JOA

Article: 12748

Dear Author,

During the copyediting of your manuscript the following queries arose.

Please refer to the query reference callout numbers in the page proofs and respond to each by marking the necessary comments using the PDF annotation tools.

Please remember illegible or unclear comments and corrections may delay publication.

Many thanks for your assistance.

Query reference	Query	Remarks
1	**AUTHOR: Please confirm that given names (red) and surnames/family names (green) have been identified correctly.**	
2	**AUTHOR: Please check that authors and their affiliations are correct.**	
3	**AUTHOR – please explain relevance of bold P-values?**	
4	**AUTHOR – please explain relevance of bold value?**	
5	**AUTHOR: To maintain sequential order, Tables 4, 5, 6, 7, 8 have been changed to Tables 4, 5, 6, 7, 8, 9. Please check.**	
6	**AUTHOR – please explain relevance of bold values?**	
7	**AUTHOR – please explain relevance of bold values?**	
8	**AUTHOR: Please check all your entries in Table 8.**	
9	**AUTHOR – what does asterisk refer to?**	
10	**AUTHOR – there is not part c in Fig. 7?**	
11	**AUTHOR – there is not part d in Fig. 7?**	
12	**AUTHOR – please explain relevance of bold values?**	
13	**AUTHOR: Nelson (1997) has not been cited in the text. Please indicate where it should be cited; or delete from the Reference List.**	
14	**AUTHOR: Prendergast and Humphrey (2014) has not been cited in the text. Please indicate where it should be cited; or delete from the Reference List.**	
15	**AUTHOR: Please provide the volume number for reference Vidarsdottir and O Higgins (2003).**	
16	**AUTHOR: Figure 1 is of poor quality. Please check required artwork specifications at https://authorservices.wiley.com/asset/photos/electronic_artwork_guidelines.pdf**	

doi: 10.1111/joa.12748

Facial shape manifestations of growth faltering in Tanzanian children

Joanne B. Cole,[1,*] Mange F. Manyama,[2,3,*] Dejana Nikitovic,[4] Paula N. Gonzalez,[5] Denise K. Liberton,[6] Warren M. Wilson,[4] Campbell Rolian,[7] Jacinda R. Larson,[8] Emmanuel Kimwaga,[3] Joshua Mathayo,[3] Charles C. Roseman,[9] Stephanie A. Santorico,[1,10] Ken Lukowiak,[11,12] Richard A. Spritz[1] and Benedikt Hallgrimsson[8,13,14]

[1]*Human Medical Genetics and Genomics Program, University of Colorado School of Medicine, Aurora, CO, USA*
[2]*Weill-Cornell Medicine-Qatar, Doha, Qatar*
[3]*Department of Anatomy, Catholic University of Health and Allied Sciences, Mwanza, Tanzania*
[4]*Department of Anthropology and Archaeology, University of Calgary, Calgary, AB, Canada*
[5]*Instituto de Genética Veterinaria, CCT-CONICET, La Plata, Argentina*
[6]*National Institute for Dental and Craniofacial Research, Bethesda, MD, USA*
[7]*Department of Comparative Biology and Experimental Medicine, Faculty of Veterinary Medicine, University of Calgary, Calgary, AB, Canada*
[8]*Alberta Children's Hospital Research Institute, University of Calgary, Calgary, AB, Canada*
[9]*Department of Animal Biology, School of Integrative Biology, University of Illinois, Urbana, IL, USA*
[10]*Mathematical and Statistical Sciences, University of Colorado, Denver, CO, USA*
[11]*Hotchkiss Brain Institute, Cumming School of Medicine, University of Calgary, Calgary, AB, Canada*
[12]*Department of Physiology and Pharmacology, Cumming School of Medicine, University of Calgary, Calgary, AB, Canada*
[13]*Department of Anatomy and Cell Biology, University of Calgary, Calgary, AB, Canada*
[14]*McCaig Institute for Bone and Joint Health, University of Calgary, Calgary, AB, Canada*

Abstract

Variation in the shape of the human face and in stature is determined by complex interactions between genetic and environmental influences. One such environmental influence is malnourishment, which can result in growth faltering, usually diagnosed by means of comparing an individual's stature with a set of age-appropriate standards. These standards for stature, however, are typically ascertained in groups where people are at low risk for growth faltering. Moreover, genetic differences among populations with respect to stature are well established, further complicating the generalizability of stature-based diagnostic tools. In a large sample of children aged 5–19 years, we obtained high-resolution genomic data, anthropometric measures and 3D facial images from individuals within and around the city of Mwanza, Tanzania. With genome-wide complex trait analysis, we partitioned genetic and environmental variance for growth outcomes and facial shape. We found that children with growth faltering have faces that look like those of older and taller children, in a direction opposite to the expected allometric trajectory, and in ways predicted by the environmental portion of covariance at the community and individual levels. The environmental variance for facial shape varied subtly but significantly among communities, whereas genetic differences were minimal. These results reveal that facial shape preserves information about exposure to undernourishment, with important implications for refining assessments of nutritional status in children and the developmental-genetics of craniofacial variation alike.

Key words: childhood growth; complex traits; craniofacial; facial imaging; growth faltering.

Correspondence
Benedikt Hallgrimsson, Department of Cell Biology & Anatomy, Faculty of Medicine, University of Calgary, 3330 Hospital Drive NW, Calgary, T2N 4N1, AB, Canada. T: +1 403-220-3060; F: +1 403-210-3829; E: bhallgri@ucalgary.ca

*J.B.C. and M.F.M. are joint first authors.

Accepted for publication *24 October 2017*

Introduction

Phenotypic variation reflects the complex interplay of the functions of many genes in an environmental context. The human face is no exception, as facial shape is the product of complex interactions among inherited genetic effects and environmental influences throughout individual life

CE: Shobana | PE: Raja J.
Dispatch: 9.11.17 | No. of pages: 13
WILEY
JOA | 12748
Journal Code | Manuscript No.

histories. Human craniofacial shape varies with both age (ontogenetic allometry) and size (static allometry; Vidarsdottir & O Higgins, 2003). As with other phenotypic traits, growth itself is also determined by the interaction between genetic and environmental factors, with environmental factors, particularly undernutrition, causing growth faltering – reduced growth relative to age (Bogin, 1999). Growth faltering due to undernutrition has been associated with lifetime and even trans-generational health impacts, including cognitive delay, metabolic diseases and immune dysfunction (Dewey & Begum, 2011), all of which influence health and economic development (UNICEF, 2009). This is particularly evident in developing countries, such as East African countries, where 42% of children under 5 years old are considered to be malnourished (de Onis et al. 2013). While it is well known that growth affects craniofacial shape, an important question remains what effect growth faltering has on craniofacial shape.

Growth faltering is assessed using international growth standards relating stature to age, such as WHO growth standards, developed using groups living under optimal environmental conditions (Borghi et al. 2006). A problem with these standards is that stature is heritable. Therefore, it is possible for populations to differ from each other due to genetic rather than environmental differences. Geographic variation has been documented in stature-influencing genes in Europe (Turchin et al. 2012; Berg & Coop, 2014). Such differences can confound the use of international growth standards to infer growth faltering in local populations.

Malnutrition, however, has general developmental effects and multiple morphological consequences (Gonzalez et al. 2011, 2016). A combination of multiple morphological indicators may better identify individuals who were malnourished during growth than using stature in isolation. If undernutrition affects facial morphology in a predictable way, then facial morphology in combination with stature or other growth outcomes can be used to improve assessment of undernutrition in children. If facial shape varies with growth faltering, then shape deviations in the direction of this effect relative to stature provide additional information about growth status. Further, if facial shape varies in ways that are not entirely bound to stature and the developmental processes that underlie this growth are perturbed by undernutrition, facial morphology could provide a more generally applicable set of indicators than stature alone. Such a relationship would allow assessment of facial morphology in relation to stature in bioarchaeological studies, for which determination of nutrition is often a key concern (Buikstra & Ubelaker, 1994).

To date, the relationship between growth faltering due to undernutrition and craniofacial development and facial shape has only been confirmed in mice (Gonzalez et al. 2016). In the present study, we explore the interaction of growth faltering and facial shape in children from northwestern Tanzania, a country with one of the highest rates of stunting – growth outcomes that fall more than two standard deviations below international growth standard – worldwide (Black et al. 2013; de Onis, 2013). Using genomic data, growth outcomes and 3D facial images from children aged 5–19 years, we tested the hypothesis that growth faltering results in predictable facial shape effects that are attributable to environmental rather than genetic variation.

Materials and methods

Setting and study populations

We analysed cross-sectional data for height, weight, head circumference (HC) and body mass index (BMI) in children from the Mwanza region in Tanzania (Fig. 1). Between 2010 and 2014, we obtained anthropometrics and 3D facial photogrammetry for 6300 children aged 5–19 years (Fig. 2) at 26 schools in the Mwanza District. We obtained genomic data for 3605 individuals using the Illumina 2.5M+Exome SNP array. All three kinds of data were available for 2978 children. Within this sample, we analysed the 5844 children whose parents were both reported to belong to local Bantu-language groups.

We obtained various indicators of environmental differences among schools. These indicators were based on direct observation, discussions with school principals and data from the Tanzanian government. These variables are described in Table 1.

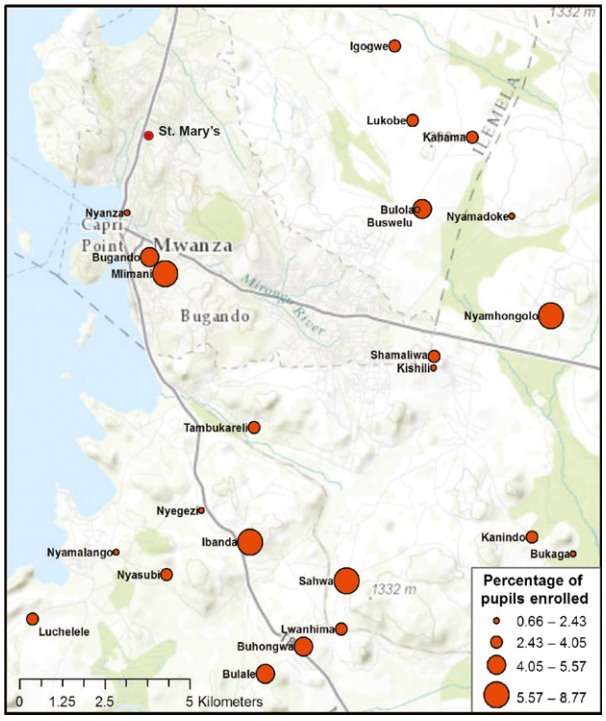

Fig. 1 Map of Mwanza. The red circles indicate school locations, and the size of the circle indicates the percentage of the overall sample collected from each school.

Investigators met with teachers and local leaders to explain the research. Consent forms, in Swahili, were provided 2 days prior to data collection. Ethics approval is by the University of Calgary (CHREB ID: 23033 and 21741) and the Tanzania National Institute of Medical Research (ID: HQ/R.8A/Vol and HQ/R.8A/Vol I.107).

This population does not exhibit significant genetic structure by school with a median fixation index (F_{ST}) across pair-wise samples of 0.0005 (Cole et al. 2016). However, there is potential for environmental variation among schools. With one exception, schools draw students exclusively from their surrounding community. The only exception is St Mary's, a private school that draws fairly high socioeconomic status students from across Mwanza. The communities from which the schools draw range from urban to rural, and in economic setting from wage-earners to subsistence farmers. While individual family histories were not obtained, a study of mobility patterns within the neighbouring Kagera regions shows that about 80% of families stayed within the same or neighbouring communities over a 13-year period before 2010 (Beegle et al. 2011).

COLOR

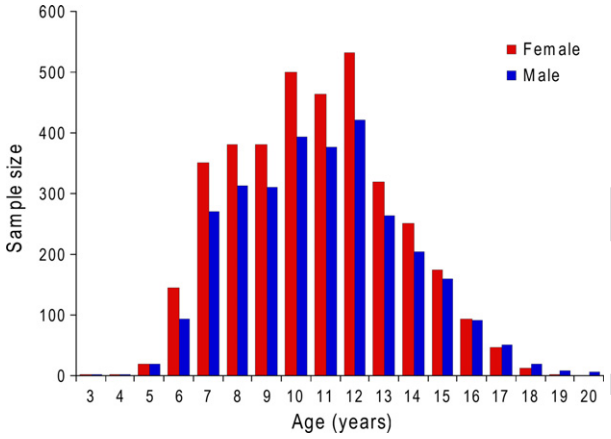

Fig. 2 Age and sex distribution of the study sample.

Anthropometrics

Weight was measured with a medical scale (Beurer BG64), height with a portable anthropometer (Seca 217), and HC with a measuring tape taken to maximize circumference from the forehead to the nuchal region above the ears. All measurements were repeated. Participants were measured without shoes wearing light clothing. Ages were self-reported.

3D facial imaging

Children were photographed using Creaform MegaCapturor II or Gemini white light 3D photogrammetry systems. Each child was imaged twice at four angles. The best images were reconstructed and assembled to produce a 3D facial surface. Landmarks were obtained via automated landmarking as described previously (Cole et al. 2016, 2017; Li et al. 2017).

Analysis of growth faltering

We used CDC growth standards (Dean et al. 2011) to calculate sex-based stature-for-age and BMI-for-age *z*-scores to assess growth of children 5–19 years old. CDC growth standards are intended to represent growth under close to ideal conditions (Kuczmarski et al. 2002). The standards for children aged 5–19 years are based primarily on US health survey data. For HC, *z*-scores were based on a US reference (Rollins et al. 2010). This standard is based on a North American population of mixed ancestry (56% African American, 39% European), and provides a more conservative assessment of faltering than previous standards (Roche et al. 1987). There are no growth standards for East African children at close to optimal growth conditions.

For most analyses, we treat growth faltering as a continuous variable as this preserves statistical power. Statistical

Table 1 Variables used to assess environmental differences among schools.

Variable	Description	Coding for CAT PCA
Local economy	Based on interviews with teachers and the principal, we classified the local economy as agricultural, wage or small-business, and mixed	Agriculture, small business and wage labour were coded as three separate binary (0,1) variables
Location	We classified schools as urban, peri-urban or rural. Schools within the city of Mwanza were coded as urban. Schools in the outer suburbs were coded as 'peri-urban', while schools in rural villages were coded as 'rural'	This factor is completely concordant with 'local economy', and so we collapsed these variables
Water source	We classified water sources by 'lake' or 'well' depending on where communities mainly obtain water	Coded as binary (0.1)
Health care facility	We classified communities as 'hospital', 'health centre' and 'dispensary' based on the type of health care facility most accessible	Coded as 0 = dispensary, 1 = health centre, 3 = hospital
Distance to health centre	This numeric variable captures the distance to the nearest health care facility in km	Treated as numeric
Proportion attending secondary school	This numeric variable is the proportion of students progressing from Form 6 to secondary school. This statistic is published for each school annually	Treated as numeric

PCA, principal components analysis.

COLOR

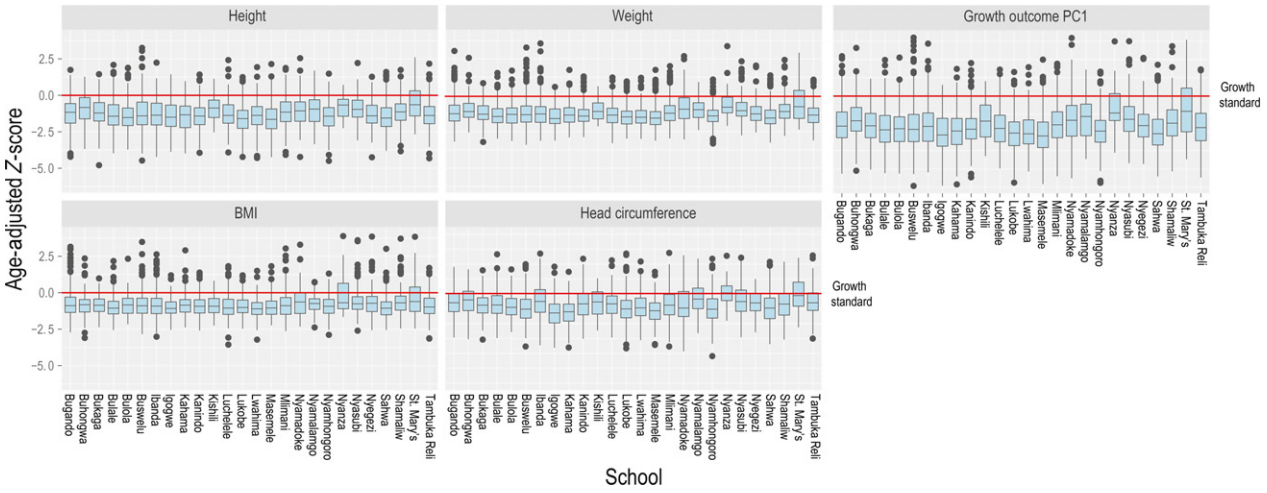

Fig. 3 Boxplots for each growth outcome by school. Variation in all growth outcomes varies significantly across schools.

Table 2 Analyses of variance by school and sex for all growth outcomes.

Variable	Effect	df	MS	*F*	*P*-value
Height	School	25	9.6	9.2	$< 1 \times 10^{-16}$
	Sex	1	80.64	80.23	$< 1 \times 10^{-16}$
	School × Sex	25	1.69	1.68	0.02
Weight	School	25	8.11	12.47	$< 1 \times 10^{-16}$
	Sex	1	50.05	76.97	$< 1 \times 10^{-16}$
	School × Sex	25	0.96	1.47	0.06
BMI	School	25	5.25	8.15	$< 1 \times 10^{-16}$
	Sex	1	24.9	38.67	5.3×10^{-10}
	School × Sex	25	0.68	1.06	0.38
HC	School	25	16.36	8.15	$< 1 \times 10^{-16}$
	Sex	1	7.1	7.12	**0.005**
	School × Sex	25	1.17	1.2	0.16
Growth PC1	School	25	29.21	15.08	$< 1 \times 10^{-16}$
	Sex	1	154.5	79.77	$< 1 \times 10^{-16}$
	School × Sex	25	3.01	1.58	

BMI, body mass index; HC, head circumference; PC, principal component.

analyses were performed in R (www.r-project.org). Individuals with *z*-scores ± 5 were identified as outliers. Given the non-linear relationship between *z*-scores and age, we normalized to age using a polynomial fit.

To obtain an overall measure of growth faltering, we performed principal components analysis (PCA) of the *z*-score data for height, weight and HC. The first component (PC1), which explains 81% of the variation among these three growth variables, was used as a summary measure of growth outcomes.

To determine whether variation in growth outcomes among school is associated with differences in the local environments, we associated variation in the first PC1 of growth outcomes with variation in available environmental variables. These variables are not intended to provide a complete explanation of the causes of variation in growth faltering among the communities included in this study. However, they can provide evidence that there is environmental variation among the communities that correlates with growth outcomes. Here, we performed an analysis of variance for the first PC of growth outcomes by all environmental variables and their interactions. Further, we analysed the full set of environmental indicators using the approach of Filmer & Pritchett (2001) in which the categorical variables are broken down into binary alternatives, represented as 0s and 1s, and then subjected to a PCA. Using mean values by school, we then examined the correlation between the first PC of growth outcomes and the first PC of the environmental variables. In this test, school rather than the individual is the unit of analysis.

Analysis of facial shape

We used geometric morphometric methods to determine the relationship between growth outcomes and facial shape. Landmark data were first corrected for reconstruction artefacts and differences between cameras. To quantify the association of growth variables to craniofacial shape, we used multiple multivariate regressions in R (Geomorph; Adams et al. 2014). To compare groups with or without covariates, we used linear models as implemented in Geomorph in R (Adams et al. 2014). Sex was included as a factor in all analyses as there are small but significant differences among male and female children of all ages (Rosas & Bastir, 2002; Bulygina et al. 2006).

Calculation of environmental variance

We determined genotypic values and environmental deviations for facial shape using genome-wide complex

Table 3 The mean height-for-age and BMI-for-age *z*-scores based on the CDC growth standards, after adjustment for age variation, for each school in the study.

		Height		Weight		HC		BMI		Growth PC1	
N	School	Mean	St. Dev.	Mean	St. Dev.	Mean	St. Dev.	Mean	St. Dev.	Mean	St. Dev.
154	Bukaga	0.05	0.92	0.02	0.70	0.48	0.86	0.38	0.69	−0.75	1.17
394	Bulale	−0.11	1.04	−0.13	0.74	0.57	0.91	0.23	0.67	−0.93	1.32
168	Igogwe	−0.16	1.11	−0.13	0.86	−0.06	0.96	0.35	0.68	−1.25	1.28
266	Kahama	−0.17	0.97	−0.05	0.73	−0.02	0.92	0.44	0.71	−1.07	1.21
178	Kanindo	−0.13	0.98	−0.05	0.76	0.53	0.97	0.37	0.72	−0.84	1.28
241	Lukobe	−0.33	0.97	−0.23	0.71	0.24	1.03	0.31	0.66	−1.22	1.20
205	Lwahima	−0.21	1.04	−0.25	0.70	0.38	0.96	0.12	0.64	−1.15	1.31
279	Masemele	−0.34	1.02	−0.18	0.75	0.15	0.83	0.39	0.67	−1.26	1.29
89	Ngasaro	0.25	0.95	0.41	1.03	0.76	1.00	0.85	1.17	−0.18	1.48
168	Nyamadoke	0.18	1.12	0.14	0.97	0.41	1.18	0.48	0.94	−0.43	1.44
669	Nyamhongoro	−0.24	0.97	−0.17	0.74	0.22	0.98	0.28	0.68	−1.02	1.19
294	Nyasubi	0.34	0.90	0.34	0.87	0.78	0.98	0.64	0.94	−0.24	1.35
515	Sahwa	−0.17	1.01	−0.14	0.77	0.32	0.99	0.26	0.73	−1.11	1.31
124	Buhongwa	0.28	0.91	0.19	0.82	0.77	0.94	0.48	0.85	−0.48	1.34
141	Bulola	−0.06	1.05	−0.04	0.80	0.28	0.84	0.31	0.75	−0.79	1.32
338	Buswelu	−0.04	1.16	0.05	0.99	0.30	0.97	0.48	0.91	−0.74	1.55
549	Ibanda	−0.08	1.07	−0.01	0.88	0.76	1.02	0.39	0.85	−0.76	1.47
48	Kishili	0.23	0.91	0.13	0.66	0.62	0.92	0.40	0.61	−0.60	1.26
232	Luchelele	−0.06	0.97	−0.05	0.74	0.59	0.95	0.34	0.84	−0.88	1.34
80	Nyamalamgo	0.21	1.06	0.24	0.93	0.99	1.16	0.53	0.69	−0.39	1.51
96	Nyegezi	−0.03	0.91	0.08	0.83	0.60	0.80	0.56	1.00	−0.63	1.29
232	Shamaliwa	0.08	0.93	0.17	0.81	0.54	0.98	0.57	0.92	−0.52	1.30
259	Tambuka_reli	−0.21	1.00	−0.13	0.76	0.79	0.96	0.36	0.78	−0.98	1.29
379	Bugando	−0.02	1.05	0.07	0.87	0.62	0.91	0.51	0.96	−0.71	1.39
322	Mlimani	0.25	0.95	0.14	0.85	0.45	1.08	0.31	0.88	−0.42	1.42
21	Nyanza	0.43	0.80	0.62	1.28	1.37	1.07	1.04	1.57	0.27	1.76
119	St Mary's	0.80	1.15	0.91	1.45	1.31	1.15	0.91	1.37	0.75	1.93

Schools are organized by location. For each school, we list the mean and standard deviation for *z*-scores for height-for-age and BMI-for-age.
BMI, body mass index; HC, head circumference; PC, principal component.

Table 4 Analysis of variance on school means for Growth Outcome PC1 by School environmental factors.

Factor	df	Sum Sq.	Mean Sq.	*F*-value	Pr (> *F*)
Local economy	2	2.09633	1.04817	6.4131	**0.007442**
Water source	2	0.14954	0.07477	0.4575	0.639667
Health care infrastructure	2	0.09414	0.04707	0.288	0.752987
Local economy by water source	1	0.4248	0.4248	2.5991	0.123409
Local economy by health care	1	0.17611	0.17611	1.0775	0.312278
Water source by health care	1	0.02275	0.02275	0.1392	0.713225
Residuals	19	3.10537	0.16344		

trait analysis (GCTA; Yang et al. 2011). With imputation, 16 million SNPs were used to calculate two genetic relationship matrices (GRMs). Using best linear unbiased prediction to estimate the corresponding variance components, the first matrix captures genetic effects of all typed and imputed SNPs, while the second captures genetic effects among close relatives. The sum of the two variance components represents an estimate of narrow sense heritability and was used to estimate genotypic values. The environmental deviation is the difference between the phenotypic and genotypic values.

For the facial landmarks, we symmetrized the landmark data and estimated the genetic variances and covariances between the pair-wise landmark combinations using the two GRMs. This results in pair-wise estimates of the genetic variances and covariance by *x*-, *y*- and *z*-coordinate of each landmark. These matrices were then used to calculate principal components and principal component scores for each individual as well as the full set of genotypic values and environmental deviations for each landmark coordinate.

COLOR

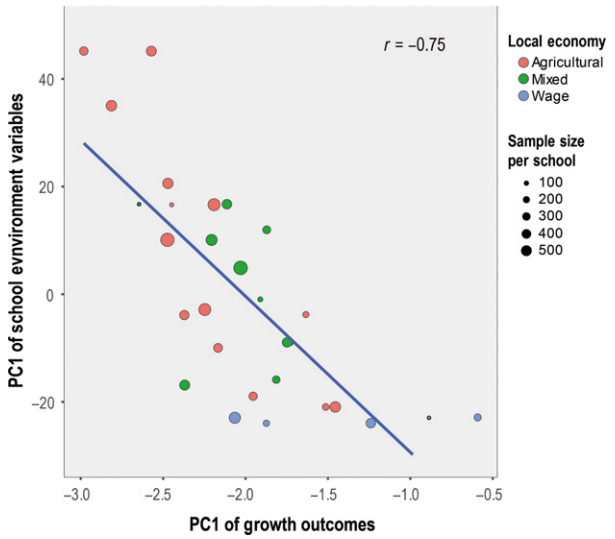

Fig. 4 Scatterplot for school means for principal component (PC)1 of school environmental variables against PC1 of growth outcomes. Points are colour-coded by local economy type, and the size of each point depicts the sample size at each school. The relationship is significant ($r = -0.76$, $P < 1 \times 10^{-6}$).

Results

Variation among communities

We compared growth outcomes among schools. School age compositions varied (ANOVA, df = 26/6504, $F = 32$, $P < 2 \times 10^{-16}$), so we normalized to age using a three-term polynomial fit. All growth outcome variables varied significantly among schools ($P < 2 \times 10^{-16}$; Fig. 3; Tables 2 and 3).

Table 5 MANOVA table for analysis of facial shape variation among schools.

Effect	df	MS	R^2	F	Z	P-value
School	24	0.009	0.017	4.2	4.0	**< 0.0001**
Sex	1	0.092	0.008	44.1	24.3	**< 0.0001**
Age	1	0.333	0.028	160.1	30.8	**< 0.0001**
School × Age	24	0.003	0.007	1.6	1.6	**< 0.0001**
School × Sex	24	0.002	0.005	1.1	1.1	0.19
Total	5524					

To determine whether variation in growth outcomes among schools related to differences in environmental conditions among schools, we performed an ANOVA for growth outcomes by the factors listed in Table 1. These results, in Table 4, show that average growth outcomes by school vary significantly by local economy (wage, mixed or agriculture) or setting (urban, peri-urban and rural). These two variables correlate perfectly across schools and so could not be disentangled. To investigate this further, we converted the environmental variables as described in Table 1 and performed a categorical PCA to reduce the environmental variables. PC1 is driven largely by scholastic outcomes, while PC2 is driven by distance to water source and distance to health centre. PC1 correlates significantly with all growth outcomes.

COLOR

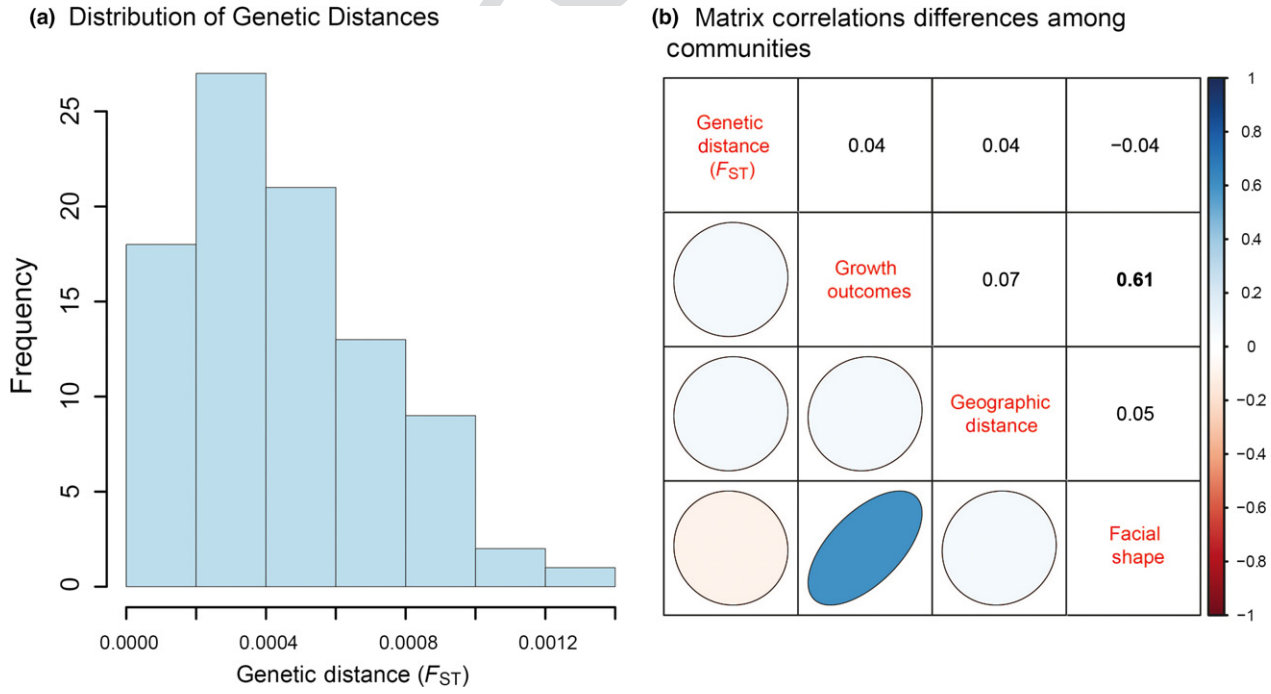

Fig. 5 Analysis of genetic distances among school. (a) Histogram of F^{ST} values for pair-wise distances between schools. (b) Matrix correlations for pair-wise genetic distances, differences in growth outcomes, geographic distances and mean differences in facial shape. Only the matrices of growth outcome and facial shape distances are significantly associated ($P < 0.001$, Mantel's permutation test, 999 iterations).

Figure 4 shows the relationship between the school environment PC1 and growth outcome PC1. These results indicate that there are environmental differences among schools that plausibly relate to variation in growth outcomes.

Table 6 MANOVA table for analysis of shape correlates of growth, age and size.

Variable	df	MS	R^2	F	Z	Prob.
Age	1	0.41	0.031	184.0	26.1	< **0.001**
Facial size	1	0.33	0.025	149.7	25.9	< **0.001**
Height (cm)	1	0.08	0.006	34.6	20.1	< **0.001**
Growth PC1	1	0.18	0.014	81.6	24.8	< **0.001**
Sex	1	0.10	0.008	45.4	22.0	< **0.001**
Age × Growth PC1	1	0.02	0.001	6.6	5.9	< **0.001**
Sex × Growth PC1	1	0.01	0.000	2.0	1.8	0.0328
Total	5524					

7 PC, principal component.

Genetic differences among schools, as measured by F_{ST}, are shown in Fig. 5a. The differences are very small, averaging 0.00045. As determined by the Mantel's permutation test, genetic distances among schools are uncorrelated with either geographic distance (r^2 = 0.0016, P = 0.51) or differences in growth outcomes (r^2 = 0.0012, P = 0.82; Fig. 5b). These results strongly suggest the absence of geographically patterned genetic variation among the communities included in the study.

Facial shape varies subtly but significantly among schools, as determined by MANOVA considering age, sex and their interactions with school (Table 5). These differences in facial shape among schools do not correlate with genetic distance. However, the differences in facial shape do correlate strongly with differences in growth outcomes among communities (R = 0.61, P < 0.001, Mantel test; Fig. 5b). Subtle differences in facial shape among the children of different communities thus correlate strongly with differences in growth outcomes but not with genetic distance.

5

COLOR

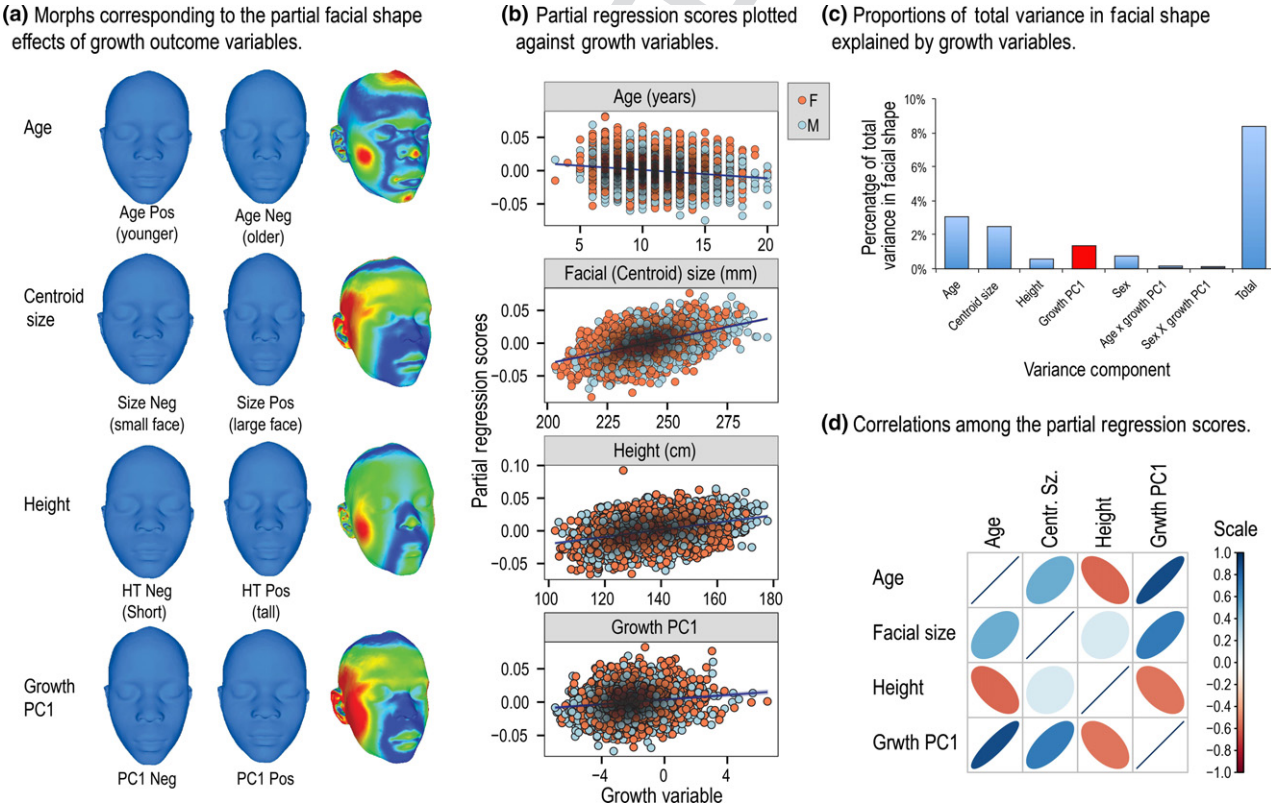

Fig. 6 The relationship between growth faltering and facial shape. (a) 3D morphs corresponding to the partial regression scores for age, facial size, height for age, and growth faltering. Note that the slope for facial shape on age is negative and so the morphs are reversed so as to correspond to others in the columns. (b) Partial regression scores plotted for each growth variable. All growth variables are significantly related to facial shape as determined by multiple multivariate regression and permutation test as described by Collyer et al. (2015) (P < 0.001 with 1000 iterations). (c) The proportions of the total variance for facial shape explained by the model and by each growth variable. (d) Directions and magnitudes of correlations among the partial regression scores. The direction of facial shape variation for height-for-age is opposite to that of the other variables.

Growth faltering and craniofacial shape

We tested the individual-level relationship between growth faltering and craniofacial shape using geometric morphometric analysis of 3D facial shape images. Specifically, we fit a multiple multivariate regression model using the procD.lm function in R (Geomorph; Adams et al. 2014). Our model considered age, facial size (centroid size), height, faltering (PC1 of *z*-scores), sex, and the interactions between all variables and age. All effects were significant at $P < 0.001$ based on the permutation test described by Collyer et al. (2015) (Table 6). These results show that growth faltering, or growth relative to age, independently relates to facial shape.

To determine the specific facial shape effects related to growth faltering, we obtained partial regression scores for each variable from this same linear model (Drake & Klingenberg, 2008). The facial shape variation that corresponds to each partial regression is shown in Fig. 6a. The full model explains 8.4% of the total variance in facial shape. From this total, 3% is due to age, 2.5% to facial size, 1% to height and 1.4% to growth faltering (growth PC1; Fig. 5c).

The partial regression scores for age, facial size and growth faltering correlate positively with each other, but negatively with the partial regression scores for stature (Fig. 6d). This can be seen in the facial shape morphs in Fig. 6a. The implication is that faltering produces variation that falls along both ontogenetic and static allometry, but

COLOR

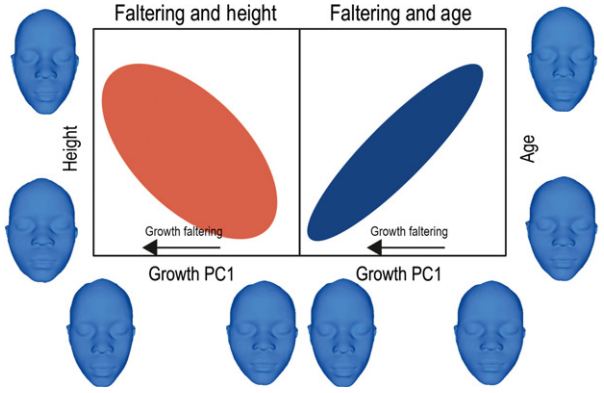

Fig. 7 Illustration of how facial shape relates to variation in stature and age. This schematic is based on the relationships shown in Fig. 5.

COLOR

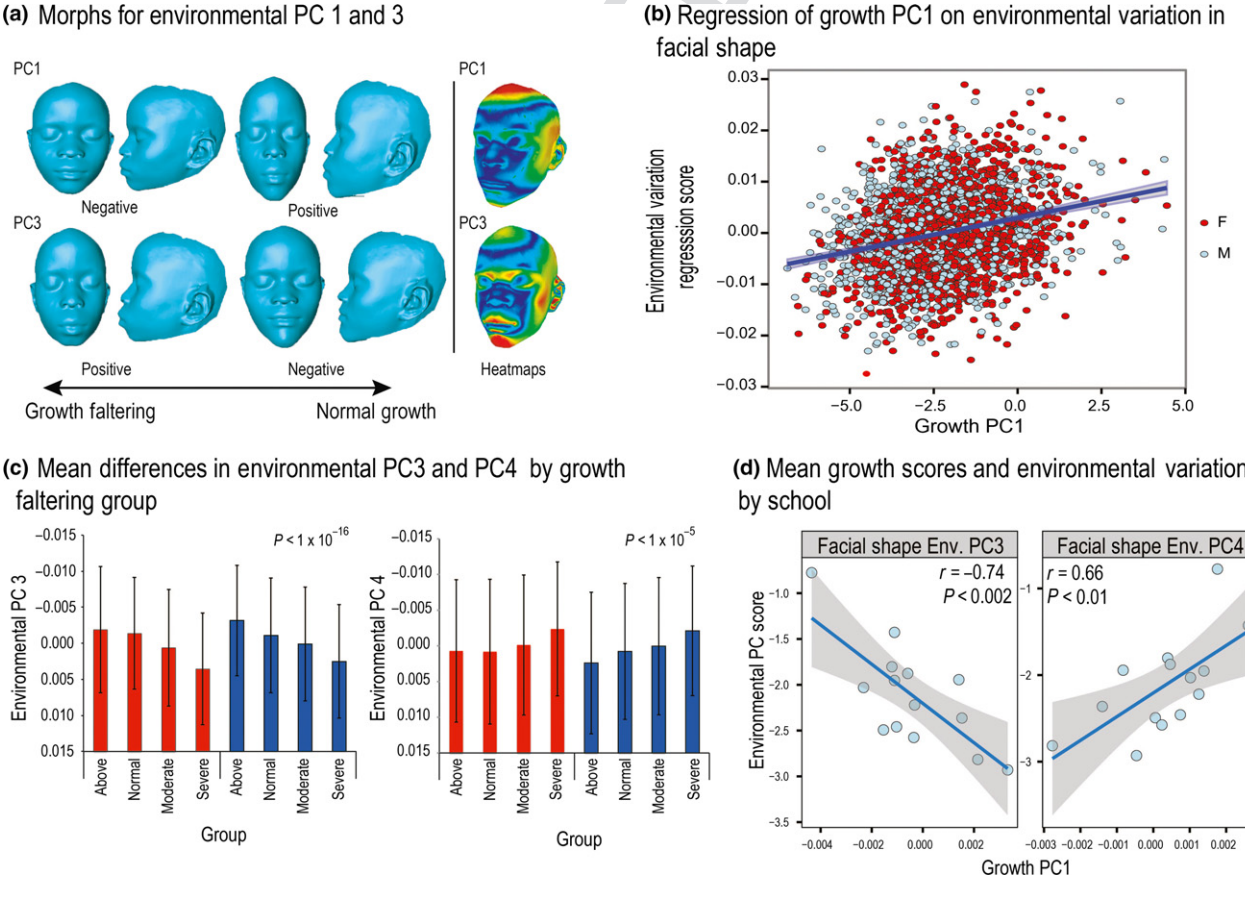

Fig. 8 Environmental variance for facial shape and growth faltering. (a) 3D morphs for environmental principal components (PCs) 1 and 3. (b) Regression of growth faltering (growth PC1) on the mean-centred environmental residual landmark data. (c) Means for environmental PCs3 and 4 by growth faltering group. (d) School means for PC3 and PC4 against school means for growth PC1.

Table 7 MANOVA table for comparison of environmental variation in facial shape across schools.

Effect	df	SS	MS	R^2	F	Z	P-value
School	18	0.015	0.00084	0.008	1.605	1.593	< 0.0001
Sex	1	0.000	0.00001	0.000	0.013	0.012	1
School × Sex	18	0.009	0.00050	0.005	0.953	0.953	0.6118
Residuals	3433	1.787	0.00052				
Total	3470	1.811					

Sex had been removed as an effect prior to the GCTA, so its main effect is expected to be 0.

COLOR

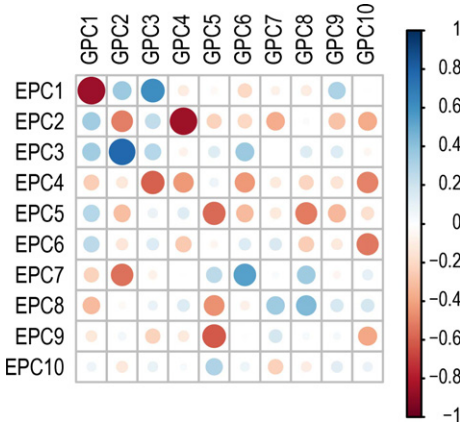

Fig. 9 Visualization of correlations between environmental and genetic principal components (PCs).

in opposite directions. Children with faltering have faces that correspond to expected facial shapes of taller and older children (Fig. 7).

Environmental vs. genetic variance

We partitioned facial shape variation using GCTA into environmental and additive genetic components. We obtained the environmental variation in facial shape by centring the environmental deviations on the mean landmark configuration. Figure 8a shows morphs of PC1 and PC3 for facial shape based on these data. School accounts for a small but significant amount of variation in the environmental component of facial shape (Table 7). We then tested the hypothesis that faltering correlates with environmental variation in facial shape at the individual level, by regressing growth PC1 on the environmental residual landmark data. Here, we tested both the individual effects of growth PC1 and also its partial effects when age, height, centroid size and weight are considered (Fig. 8b). Environmental variation in facial shape correlates significantly with faltering at $P < 0.0001$ (Procrustes MANOVA with 10 000 random permutations).

To examine the relationship between genetic and environmental covariance structure, we obtained the matrix of correlations among all genetic and environmental PCs (Fig. 9), as well as the matrix correlation between the environmental and genetic variance–covariance matrices. The matrix correlation is 0.584 ($P < 0.001$, Mantel's test with 1000 permutations). The first 10 environmental PCs all show some level of correlation with genetic PCs (Table 8), confirming the positive association of genetic and environmental covariance structure.

To determine the components of environmental facial shape variation affected by growth faltering, we regressed environmental PCs for facial shape on faltering (Table 9), which showed that PCs 1, 3 and 4 vary significantly with faltering when age and sex are considered. Dividing the sample into four categories based on level of faltering showed that PC3 and PC4, in particular, vary significantly among growth faltering categories (Fig. 7c). Remarkably, the mean values for these components of environmental facial shape variation in each of the 14 schools correlate very strongly with the mean growth outcomes of the schools for which full genomic and growth data were available. Together, environmental PC3 and PC4 explain about half the variation in growth outcomes among these schools (Fig. 7d). These results suggest that variation in growth outcomes among schools is predominantly environmental in origin and not due to genetic relatedness of the children in schools. This is consistent with the overall low level of genetic differentiation among schools.

Discussion

This analysis of the relationship between growth faltering and facial shape in Tanzanian schoolchildren reveals a unique and quantifiable axis of facial shape variation that results from environmental rather than genetic variation. The degree of growth faltering varies among schools. Further, schools vary in environmental factors that plausibly relate to variation in growth faltering. We quantified facial shape variation that corresponds to age, facial size, height and faltering, and found that they explain over 8% of the total facial shape variance. The facial shape effects of faltering correlate positively with age (ontogenetic allometry), but negatively with height (static allometry). This means that individuals with growth faltering have facial shapes that correspond to those expected in older, but taller children (Fig. 7). Specifically, in terms of ontogenetic allometry,

8 **Table 8** ANOVA tables for analysis of school variation with age fitted to three-term polynomial function.

	df	Sum Sq.	Mean Sq.	*F*-value	Pr (> *F*)
Growth PC1					
School	26	994.7	38.26	21.2418	< 2e-16
Sex	1	157.1	157.07	87.215	< 2e-16
Poly(age)	3	1131.5	377.17	209.4233	< 2e-16
School : Sex	26	59.1	2.27	1.2618	0.1685
Residuals	6340	11 418.2	1.8		
Height					
School	26	454.1	17.47	17.279	< 2e-16*
Sex	1	123.2	123.25	121.928	< 2e-16*
Poly(age)	3	983.4	327.80	324.288	< 2e-16*
School : Sex	26	37.4	1.44	1.423	0.07538
Residuals	6497	6567.4	1.01		
Weight					
School	26	370.2	14.237	20.4632	< 2e-16*
Sex	1	76.9	76.916	110.5559	< 2e-16*
Poly(age)	3	482.2	160.748	231.051	< 2e-16*
School : Sex	26	24.9	0.959	1.3786	0.0952
Residuals	6499	4521.5	0.696		
HC					
School	26	567.5	21.828	23.7374	< 2.20E-16
Sex	1	20.5	20.527	22.3225	23.57E-07
Poly(age)	3	166.1	55.359	60.2030	< 2.20E-16
School : Sex	26	34.9	1.342	1.4589	0.06202
Residuals	6099	5608.3	0.92		
BMI					
School	26	176	6.770	10.3213	< 2.20E-16
Sex	1	40.1	40.127	61.1711	66.60E-17
Poly(age, 3)	3	128.2	42.721	65.1259	< 2.20E-16
School : Sex	26	23.2	0.89	1.3574	0.1061
Residuals	6492	4258.6	0.656		

9 BMI, body mass index; HC, head circumference; PC, principal component.

Table 9 Multiple linear regression of growth faltering on environmental PCs.

Effect	Estimate	Std. err	*t*	Prob.
Model	−0.9	0.13	−7.1	**$< 1 \times 10^{-12}$**
PC1	6.6	2.22	3.0	**0.0030**
PC2	1.56	2.51	0.6	0.53523
PC3	−41.7	3.08	−13.5	**$< 2 \times 10^{-16}$**
PC4	−16.8	3.93	−4.3	**$< 2 \times 10^{-5}$**
PC5	2.3	4.56	0.5	0.61896
Age	−0.1	0.01	−8.7	**$< 2 \times 10^{-16}$**
Sex	1.5	0.20	7.5	**$< 8 \times 10^{-14}$**
Age × Sex	−0.2	0.02	−9.9	**$< 2 \times 10^{-16}$**

12 PC, principal component.

faltering dissociates the growth trajectories for stature and facial shape such that individuals with faltering have the expected faces of individuals that are further along the ontogenetic trajectory for facial shape. In terms of static allometry, it shifts the expected facial shapes relative to stature downwards.

But how does faltering result in a face that resembles those of taller but older children? Previous work in animal models has shown that brain size is less affected by nutritional stress than either somatic or facial growth, altering the ratio of brain to facial size (Gonzalez et al. 2016). This is evident in human data as well (Baker et al. 2010). An individual that has *z*-scores below 2 standard deviations of growth standards for both stature and HC will have a brain that is 10% larger relative to stature than an individual whose *z*-score is 2 standard deviations above the mean. The surprising result from our analysis is that growth faltering produces variation in the opposite direction of this overall trend. Our analyses showed that children with faltering have relatively higher, narrower and more prognathic faces. This finding suggests that the developmental trajectories for somatic growth and the face are partially dissociated by growth faltering.

Our present study and results are subject to the limitation that, as birth registration and hospital birth rates are low in Tanzania (16% and 41%, respectively), particularly in the poorest communities, all ages in our sample

are self-reported. Errors in self-reported age can be both random and biased. Random variation would decrease the estimate of the facial shape correlated with growth faltering as well as the genetic component of growth relative to age. The heritability of stature in our sample is 0.48 (Cole et al. 2017), which is low compared with that estimated from North American or European populations, which range from 0.6 to 0.9 (Mueller, 1976), but is fairly similar to estimates from other Sub-Saharan African populations (0.58; Roberts et al. 1978). Increased environmental variance due to variation in growth faltering will reduce heritabilities, but random error in the age estimates will reduce it further. To the extent that there is random variation in age in our sample, this will bias against rejecting the null hypothesis that growth faltering and facial shape are unrelated as it will introduce noise into the analysis, making it more difficult to detect the effect of faltering. Self-reported ages can result in bias if the children in the sample are older or younger than reported, on average. In our sample this would likely bias towards older self-reported age compared with actual age. A study of social determinants of school-attendance in north-western Tanzania document strong social biases that decrease or delay school attendance, such as the need to pay tuition, supply uniforms and materials, and the need for children to perform agricultural and household work (Burke & Beegle, 2004). Therefore, it is unlikely that many children will be sent to school at an earlier age than required by law. If this bias exists in our sample, it would lead to underestimates of the degree of growth faltering and this would also bias against finding the results we have reported here.

The results of our study show that the covariance structures of the environmental deviations and genotypic values are fairly similar. This is consistent with Cheverud's conjecture that genetic and environmental effects tend to produce phenotypic effects via the same developmental processes (Cheverud, 1982). For example, if genetic and environmental factors both influence the growth of cartilage, then variation in cartilage growth, whether of genetic or environmental origin, might result in a similar pattern of covariation. Our finding that growth faltering acts along the shape trajectories that define both static and ontogenetic allometry, but in the opposite direction, is consistent with this.

This finding also underscores the complex role that size and scaling plays as a determinant of morphological variation. Allometric variation is a frequently reported pattern of morphological variation, but its mechanistic basis is poorly understood. Brain size and chondrocranial growth account for significant proportions of craniofacial shape variation in both humans and mice (Martínez-Abadías et al. 2012). Brain and chondrocranial size relate allometrically but differently to both body size and facial size in most vertebrates (Strait, 1999; Hallgrimsson et al. 2007; Marcucio et al. 2011; Marugán-Lobón et al. 2016), and both factors affect craniofacial shape (Boughner et al. 2008; Hallgrímsson et al. 2009; Marcucio et al. 2011). These scaling relationships predict that taller individuals tend to have smaller brains relative to facial size and stature. Our results point strongly toward variation in the relative growth of the brain and chondrocranium as the mechanistic basis for allometric variation in facial shape. The differential scaling of central mechanisms that drive variation in complex structures such as the craniofacial skeleton is likely to be a general developmental explanation for allometry in complex traits.

Our finding that growth faltering alters the allometric relationship between facial shape and stature has several practical implications. The skeletal remains of past populations are key sources of information about health, including nutritional status (Larsen, 2002). Surface facial shape from 3D imaging and underlying skeletal morphology are very highly correlated (Young et al. 2016). Our results suggest that differences in face-stature allometry across time or among related groups may provide evidence for differences related to growth faltering. For population health, our finding that growth faltering affects the facial morphology in a predictable way suggests it is possible to use the facial shape in relation to stature to improve assessment of health status and malnutrition in children when compared with the use of stature alone. Our approach is non-invasive and we have automated phenotypic assessment to allow rapid collection of large datasets (Li et al. 2017). Individual growth outcomes have complex determinants. The novel dimension of automated facial shape assessment is thus very likely to improve the resolution and reliability of assessment of growth faltering from anthropometric data.

Acknowledgements

Many people participated in various aspects of the Facebase Tanzania project, of which this study is part. Megan Wright, Maria Finnsdóttir, Kimia Ghavami, Jared Spitzmacher, Tracey Ferrara and Sheri Riccardi contributed to reconstruction of the facial image data. Sariko Matari and Saleh Seleman Mganzil, Mitzi Murray, John Humphreys, Heather Jamnizcky, Campbell Rolian, Kai Lukowiak, Kris Kannon, Hayley Britz, Rebecca Green, Kim McKenney, Kimani Leyaro, Margaret Kaisoe, Diana Dills, Nicola Hahn, Elizabeth Hallgrímsson, Kristján Benediktsson, Elizabeth Hurst and Leigh Hurst assisted in the field. The authors also thank the teachers in the many schools in which this work was conducted and, most importantly, the children who participated as well as their parents. Primary data were deposted at dbGaP (http://www.ncbi.nlm.nih.gov/gap, accession: phs000622.v1.p1) and FaceBase (https://www.facebase.org/, accession: FB00000667.01). The authors have no conflicts of interest to declare.

Author contributions

BH, KL, MM, WW and RS designed the study. BH, JC, DL, ML, JL, PG, SS and CCR performed the data analysis. JC performed the analysis of genomic data. BH, PG and CCR

performed morphometric analysis. DL, BH, JC, DN and WW performed analyses of growth data. MM, KL, BH, WW, DL, JL, SM, JM, EK, CR and RS performed primary data collection. MM, CR, BH and WW designed the data collection system. MM and KL provided logistical support. BH, DN, JB, KL, CCR and RS wrote the paper with substantial input from MM and JC. All authors commented on drafts.

Funding

This study was supported by NIH-NIDCR (U01DE020054) to RS and BH, NSERC Grant #238992-12 to BH, and University of Calgary (UIRG to MM, KL and BH).

References

Adams DC, Collyer ML, Otarola-Castillo E, et al. (2014). Geomorph: Software for Geometric Morphometric Analyses. R package version 2.1. http://cran.r-project.org/web/packages/geomorph/index.html

Baker J, Workman M, Bedrick E, et al. (2010) Brains versus brawn: an empirical test of Barker's brain sparing model. *Am J Human Biol* **22**, 206–215.

Beegle K, De Weerdt J, Dercon S (2011) Migration and economic mobility in Tanzania: evidence from a tracking survey. *Rev Econ Stat* **93**, 1010–1033.

Berg JJ, Coop G (2014) A population genetic signal of polygenic adaptation. *PLoS Genet* **10**, e1004412.

Black RE, Victora CG, Walker SP, et al. (2013) Maternal and child undernutrition and overweight in low-income and middle-income countries. *Lancet* **382**, 427–451.

Bogin B (1999) *Patterns of Human Growth*. Cambridge: Cambridge University Press.

Borghi E, De Onis M, Garza C, et al. (2006) Construction of the World Health Organization child growth standards: selection of methods for attained growth curves. *Stat Med* **25**, 247–265.

Boughner JC, Wat S, Diewert VM, et al. (2008) Short-faced mice and developmental interactions between the brain and the face. *J Anat* **213**, 646–662.

Buikstra JE, Ubelaker DH (eds) ((1994) *Standards for Data Collection from Human Skeletal Remains*. Fayetteville: Arkansas Archeological Survey Research Series No. 44.

Bulygina E, Mitteroecker P, Aiello L (2006) Ontogeny of facial dimorphism and patterns of individual development within one human population. *Am J Phys Anthropol* **131**, 432–443.

Burke K, Beegle K (2004) Why children aren't attending school: the case of Northwestern Tanzania. *J African Econ* **13**, 333–355.

Cheverud JM (1982) Phenotypic, genetic, and environmental integration in the cranium. *Evolution* **36**, 499–516.

Cole JB, Manyama M, Kimwaga E, et al. (2016) Genomewide association study of African children identifies association of SCHIP1 and PDE8A with facial size and shape. *PLoS Genet* **12**, e1006174.

Cole JB, Manyama MF, Larson JR, et al. (2017) Heritability and genetic correlations of human facial shape and size. *Genetics* **205**, 967–978.

Collyer ML, Adams DC, Otarola-Castillo E, et al. (2015) A method for analysis of phenotypic change for phenotypes described by high-dimensional data. *Heredity* **115**, 357–365.

Dean AG, Arner TG, Sunki GG (2011). Epi InfoTM, a database and statistics program for public health professionals (computer program).

Dewey KG, Begum K (2011) Long-term consequences of stunting in early life. *Matern Child Nutr* **7**, 5–18.

Drake AG, Klingenberg CP (2008) The pace of morphological change: historical transformation of skull shape in St Bernard dogs. *Proc Biol Sci* **275**, 71–76.

Filmer D, Pritchett LH (2001) Estimating wealth effects without expenditure data – or tears: an application to educational enrollments in states of India. *Demography* **38**, 115–132.

Gonzalez PN, Edith Oyhenart E, Hallgrimsson B (2011) Effects of environmental perturbations during postnatal development on the phenotypic integration of the skull. *J Experim Zool Part B-Mol Develop Evolut* **316B**, 547–561.

Gonzalez PN, Gasperowicz M, Barbeito-Andrés J, et al. (2016) Chronic protein restriction in mice impacts placental function and maternal body weight before fetal growth. *PLoS ONE* **11**, e0152227.

Hallgrimsson B, Lieberman DE, Liu W, et al. (2007) Epigenetic interactions and the structure of phenotypic variation in the cranium. *Evol Dev* **9**, 76–91.

Hallgrimsson B, Jamniczky H, Young NM, et al. (2009) Deciphering the palimpsest: studying the relationship between morphological integration and phenotypic covariation. *Evol Biol* **36**, 355–376.

Kuczmarski RJ, Ogden CL, Guo SS, et al. (2002) 2000 CDC Growth Charts for the United States: methods and development. Vital and health statistics. Series 11. *Data National Health Survey* **246**, 1–190.

Larsen CS (2002) Bioarchaeology: the lives and lifestyles of past people. *J Archaeol Res* **10**, 119–166.

Li M, Cole JB, Manyama M, et al. (2017) Rapid automated landmarking for morphometric analysis of three-dimensional facial scans. *J Anat*, **230**, 607–618.

Marcucio RS, Young NM, Hu D, et al. (2011) Mechanisms that underlie co-variation of the brain and face. *Genesis* **49**, 177–189.

Martínez-Abadías N, Mitteroecker P, Parsons TE, et al. (2012) The developmental basis of quantitative craniofacial variation in humans and mice. *Evol Biol* **39**, 554–567.

Marugán-Lobón J, Watanabe A, Kawabe S (2016) Studying avian encephalization with geometric morphometrics. *J Anat* **229**, 191–203.

Mueller WH (1976) Parent-child correlations for stature and weight among school aged children: a review of 24 studies. *Hum Biol* **48**, 379–397.

Nelson M (1997) The validation of dietary assessment. In: *Design Concepts in Nutritional Epidemiology* (eds Margetts BM, Nelson M), pp. 241–272. Oxford: Oxford University Press. 13

de Onis M (2013) Update on the implementation of the WHO child growth standards. *World Rev Nutr Diet* **106**, 75–82.

Onis M, Dewey KG, Borghi E, et al. (2013) The World Health Organization's global target for reducing childhood stunting by 2025: rationale and proposed actions. *Mater Child Nutr* **9**, 6–26.

Prendergast AJ, Humphrey JH (2014) The stunting syndrome in developing countries. *Paediatr Int Child Health* **34**, 250–265. 14

Roberts DF, Billewicz WZ, McGregor IA (1978) Heritability of stature in a West African population. *Ann Hum Genet* **42**, 15–24.

Roche AF, Mukherjee D, Guo SM, et al. (1987) Head circumference reference data: birth to 18 years. *Pediatrics* **79**, 706–712.

Rollins JD, Collins JS, Holden KR (2010) United States head circumference growth reference charts: birth to 21 years. *J Pediatr* **156**, 907–913. e902.

Rosas A, Bastir M (2002) Thin-plate spline analysis of allometry and sexual dimorphism in the human craniofacial complex. *Am J Phys Anthropol* **117**, 236–245.

Strait DS (1999) The scaling of basicranial flexion and length. *J Hum Evol* **37**, 701–719.

Turchin MC, Chiang CW, Palmer CD, et al. (2012) Evidence of widespread selection on standing variation in Europe at height-associated SNPs. *Nat Genet* **44**, 1015–1019.

UNICEF (2009). *Tracking Progress on Child and Maternal Nutrition: a Survival and Development Priority*. UNICEF.

Vidarsdottir US, O Higgins P (2003) Developmental variation in the facial skeleton of anatomically modern Homo sapiens. *Cambridge Stud Biol Evolut Anthropol*, **????**, 114–143.

Yang J, Manolio TA, Pasquale LR, et al. (2011) Genome partitioning of genetic variation for complex traits using common SNPs. *Nat Genet* **43**, 519–525.

Young NM, Sherathiya K, Gutierrez L, et al. (2016) Facial surface morphology predicts variation in internal skeletal shape. *Am J Orthod Dentofac Orthop* **149**, 501–508.

15